PIER C

(Received 28 May 2026, Accepted 20 July 2026, Scheduled 3 August 2026)

A Low-Profile Flexible UWB Wearable Antenna Loaded with Patch Slots and Defected Ground Structure for Wireless Body Area Networks

Md. Ariful Islam[1,*], Md. Masud Rana[1], Amrito Paul[1], Abdul K. M. Zakir Hossain[2], and Noor B. Asan[2]

[1]*Department of Electrical and Electronic Engineering*
Rajshahi University of Engineering and Technology, Rajshahi 6204, Bangladesh
[2]*Centre for Telecommunication Research and Innovation*
Fakulti Teknologi dan Kejuruteraan Elektronik dan Komputer
Universiti Teknikal Malaysia Melaka, Durian Tunggal, Melaka 76100, Malaysia

ABSTRACT: This study introduces a compact, low-profile ultra-wideband (UWB) wearable antenna designed for wireless body area network (WBAN) applications. The antenna incorporates a rectangular patch on a flexible jeans substrate, incorporating one patch slot, four identical edge slots, and a defected ground structure (DGS) with compact dimensions of 23 mm × 30 mm × 1.5 mm. These slots and the DGS enable UWB operation with an excellent bandwidth while maintaining a good balance among the key performance parameters such as efficiency, gain, and SAR, which is the main contribution of this study. The antenna performance was analyzed using a four-layer human body phantom model that includes skin, fat, muscle, and bone layers. It operates across the frequency range of 2.82–11.25 GHz, covering the UWB range for wearable devices, and achieves a peak gain of 3.79 dBi, an average gain of 2.36 dBi, a peak efficiency of 63.36%, and an average efficiency of 52.88%. In addition, the obtained SAR values are 0.549 W/kg and 0.391 W/kg at 5 GHz, and 0.0727 W/kg and 1.97 W/kg at 9 GHz for 1 g and 10 g tissue standards, respectively, complying with SAR regulatory standards. Moreover, bending analysis validated its stable performance under various angles and deformation conditions. The fabrication and on-body testing of the proposed antenna exhibited a bandwidth of 1.38–12 GHz, demonstrating compliance with simulations. Finally, a human body temperature monitoring prototype was developed, which validates its suitability for wearable WBAN applications.

1. INTRODUCTION

Advances in consumer electronics and wireless technology have driven wearable medical devices and physiological monitoring systems toward greater integration, higher data rates, and reduced energy consumption [1]. The inclusion of smart sensors and machine learning further demands high data rates and reliable real-time communication in Wireless Body Area Networks (WBANs) [2]. WBANs allow wearable devices to measure vital signs such as heart rate, body temperature, glucose level, blood pressure, and body weight [3–6]. They also facilitate fast communication in entertainment devices such as virtual reality, augmented reality, smart glasses, and headsets [7–9]. WBANs offer secured tracking and communication in the military field using devices such as smartwatches and helmets [10, 11]. Ultra-wideband (UWB) technology has become a promising solution for WBAN applications because of its low power consumption, low cost, and high data-rate transmission [12]. After the Federal Communications Commission (FCC) allocated the unlicensed 3.1–10.6 GHz band in 2002, UWB technology has been significantly considered for wearable communication systems. Antennas, especially UWB antennas, are key components in wearable healthcare systems because they provide reliable, high-speed, and low-interference communication [13].

Recent studies on WBAN wearable antennas have utilized circular and elliptical patch structures together with different resonant elements to achieve wide-bandwidth performance [14–17]. For example, a coplanar waveguide (CPW)-fed antenna with circular and elliptical stubs achieved operation across the 3.1–10.6 GHz range [18], while a circularly polarized antenna with an umbrella-shaped patch and a modified elliptical radiator was proposed in [19]. Moreover, slotted structure designs on the patch and ground plane enhanced the bandwidth to 3.1–13.4 GHz and 7.5–12.5 GHz, respectively [20, 21]. Although these antennas achieved good impedance bandwidth performance, many designs still have disadvantages, such as structural complexity, large size, rigid geometry, and limited suitability for medical applications.

Again, wearable antennas must be flexible, so they can adapt to different shapes and deformations. As a result, a substantial amount of research has focused on flexible UWB antennas for WBAN applications [22, 23]. Examples include a flexible UWB antenna for breast cancer detection operating at 4–6 GHz [24] and a low-profile denim-based microstrip antenna for wideband communication [25]. In addition, a flexible UWB metasurface antenna has been developed to provide high

* Corresponding author: Md. Ariful Islam (ariful.islam@eee.ruet.ac.bd).

doi:10.2528/PIERC26052801

Published by THE ELECTROMAGNETIC ACADEMY

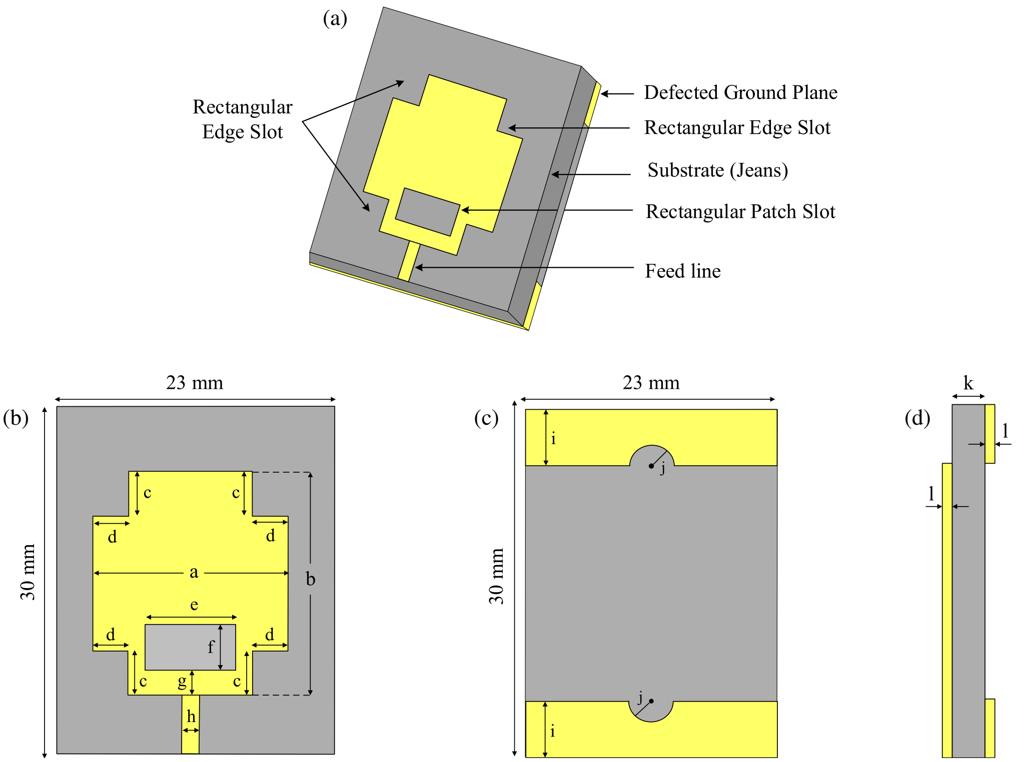

FIGURE 1. (a) Perspective view, (b) front view, (c) back view, and (e) side view of the proposed antenna design.

gain, wide bandwidth, and low SAR, enabling reliable continuous health monitoring and supporting both on-body and off-body transmission [26]. More notable designs include textile-based UWB antennas for telemedicine and mobile health, ensuring reliable on-body performance [27], ultra-miniaturized UWB patch antennas for low-interference e-health monitoring [28], four-port footwear-integrated antennas covering 2–14 GHz [29], metamaterial-enhanced textile antennas improving bandwidth and radiation efficiency [30], and miniaturized circularly polarized UWB antennas offering dual-band, body-centric communication for smart wearable devices [31]. Additionally, graphene-based flexible antennas offer high conductivity ($\approx 40 \times 10^7$ S/m) and gain (> 10 dBi) due to their excellent mechanical flexibility and nanocomposite enhancement [32, 33]. However, performance is limited by graphene's zero bandgap and fabrication complexity with strong trade-offs among size, gain, and bandwidth [34, 35]. Although existing studies have made significant improvements in wearable antenna performance, achieving low-profile, flexible, compact designs with sufficient gain, wide bandwidth, and low specific absorption rate (SAR) for reliable WBAN applications remains challenging.

This paper presents a flexible UWB wearable antenna for WBAN application. It consists of a slotted rectangular patch on a flexible jeans substrate with dimensions of 23 mm × 30 mm × 1.5 mm. The design includes a rectangular slot close to the feed line, four identical edge slots, and a defected ground structure for wideband operation while maintaining a simplified geometry. The antenna offers a peak gain of 3.79 dBi, average gain of 2.36 dBi, peak efficiency of 63.36%, and average efficiency of 52.88%. Moreover, the antenna complies with the permissible SAR standards and exhibits stable performance under bending conditions.

2. ANTENNA DESIGN METHODOLOGY

2.1. Geometry of the Proposed Antenna

The structure of the proposed antenna is shown in Fig. 1, and its optimized geometrical parameters are listed in Table 1. It is designed as a rectangular patch structure on a flexible jeans fabric substrate of 1.5 mm thickness and a dielectric constant of 1.7. Copper is used for the radiating patch and ground plane layer, with an electrical conductivity of 5.8×10^7 S/m and a thickness of 0.05 mm. The overall dimensions of the antenna were $23 \times 30 \times 1.5$ mm^3. Since the antenna has a very small thickness compared to the operating wavelength, it exhibits low-profile characteristics, making it suitable for wearable applications.

To achieve ultra-wideband operation, a slotted radiating patch and defected ground structure were incorporated into the antenna design. Furthermore, an inset-fed excitation technique

TABLE 1. Optimized geometrical parameters.

Parameter	Value (mm)	Parameter	Value (mm)
a	18.00	g	2.00
b	18.00	h	1.57
c	4.00	i	5.00
d	3.50	j	1.00
e	8.00	k	1.50
f	5.00	l	0.035

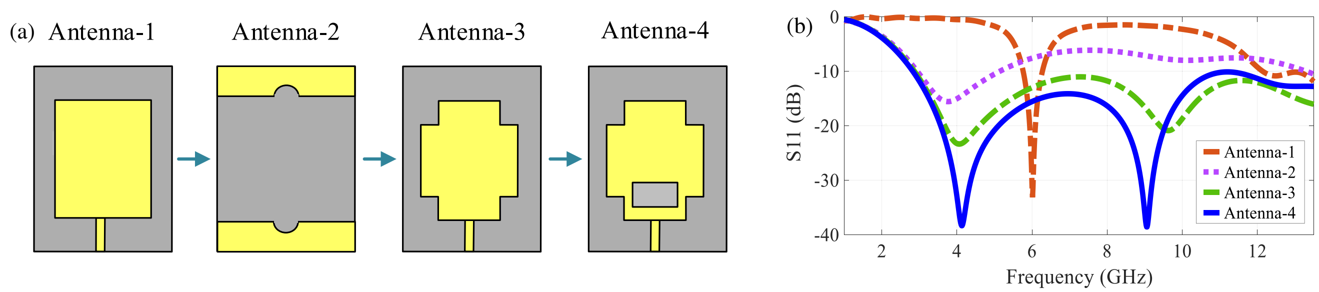

FIGURE 2. (a) Evolution steps and (b) corresponding reflection coefficient (S_{11}) results of the proposed antenna design.

was used to enhance impedance matching and optimize power transfer. The antenna design was developed and evaluated using Computer Simulation Technology (CST) Microwave Studio software to obtain the desired ultra-wideband performance.

2.2. Mathematical Modelling of the Proposed Antenna

The patch width (W) and length (L) of the proposed antenna were calculated using the following equations [36].

$$W = \frac{1}{2f_r\sqrt{\mu_0\varepsilon_0}}\sqrt{\frac{2}{\varepsilon_r+1}} \quad (1)$$

$$L = \frac{1}{2f_r\sqrt{\varepsilon_{eff}}\sqrt{\mu_0\varepsilon_0}} - 0.824h\frac{(\varepsilon_{eff}+0.3)\left(\frac{W}{h}+0.264\right)}{(\varepsilon_{eff}-0.258)\left(\frac{W}{h}+0.8\right)} \quad (2)$$

where the effective dielectric constant

$$\varepsilon_{eff} = \frac{\varepsilon_r+1}{2} + \frac{\varepsilon_r-1}{2}\left[1+\frac{12h}{W}\right]^{-1/2}$$

f_r = resonant frequency, μ_0 = permeability of free space, ε_0 = permittivity of free space, ε_r = dielectric constant of the substrate, h = height (thickness) of the substrate.

2.3. Evolution of the Antenna Structure

The evolution of the proposed antenna design is illustrated in Fig. 2. Firstly, a simple rectangular patch antenna was designed using Equations (1) and (2), which exhibited narrowband operation, resonating at 6 GHz. Next, a defected ground structure (DGS) was incorporated, which reduced the operating frequency to 3.75 GHz and increased the impedance bandwidth. To achieve the entire ultra-wideband range (3.1–10.6 GHz), four identical rectangular edge slots were etched into the radiating patch. Finally, a rectangular slot was introduced near the feed line to improve the reflection coefficient, resulting in the antenna's desired wideband performance.

2.4. Parametric Investigation of the Proposed Antenna

A detailed parametric analysis was performed to optimize performance parameters of the proposed antenna design. The effect of the patch slot length (e) on the reflection coefficient (S_{11}) is shown in Fig. 3(a). It is observed that variation in the patch slot length does not significantly affect the resonant frequencies, but rather mainly influences the magnitude of S_{11}. The optimum response was obtained at $e = 8$ mm. Fig. 3(b) shows that increasing the ground width (i) lowers the high-band frequencies. A ground width of 5 mm provided the best overall performance. In addition, the dimensions of the rectangular edge slot ($c \times d$) significantly affect the impedance bandwidth, as shown in Fig. 3(c). As the slot dimensions increase, the bandwidth narrows. The desired response was achieved for $c \times d = 4 \times 3.5\,\text{mm}^2$. Hence, good impedance matching is achieved with a patch slot length of 8 mm, ground width of 5 mm, and a dimension of the rectangular edge slot of $4 \times 3.5\,\text{mm}^2$. The optimized dimensions, along with all other geometrical parameters, are listed in Table 1.

3. RESULTS AND DISCUSSION

3.1. Numerical Analysis of the Proposed Antenna

Antennas designed for WBAN applications must exhibit stable performance of various parameters in the body-surface environment. Thus, a rectangular human body phantom model with dimensions of $80 \times 80\,\text{mm}^2$ was designed in CST Studio software, where the antenna was placed above the phantom model with a 3 mm air gap, as illustrated in Fig. 4. The human tissue properties used in the phantom model are presented in Table 2 [27]. Again, open (add space) boundary conditions were used to simulate free-space radiation, along with a hexahedral mesh having a -40 dB accuracy setting to ensure numerical precision.

TABLE 2. Properties of different layers of human body tissue.

Property	Skin	Fat	Muscle	Bone
Permittivity, ε_r (F/m)	35.93	4.90	48.49	18.49
Density (kg/m^3)	1100	910	1040	1008
Conductivity (Ωm)	3.72	0.15	4.96	0.82
Thickness (mm)	2	5	20	13

Figure 5 shows the simulated reflection coefficient (S_{11}) with respect to frequency. The results show that the proposed antenna achieves adequate impedance matching over the entire UWB range of 2.82 GHz to 11.25 GHz. The antenna achieves a wide operating bandwidth of 8.43 GHz with a fractional bandwidth of 149.67%. The average efficiency obtained across the entire operating band was 52.88%, with a peak efficiency of 63.36%, as shown in Fig. 6. This moderate efficiency is mainly attributed to dielectric losses in the jeans substrate and ohmic

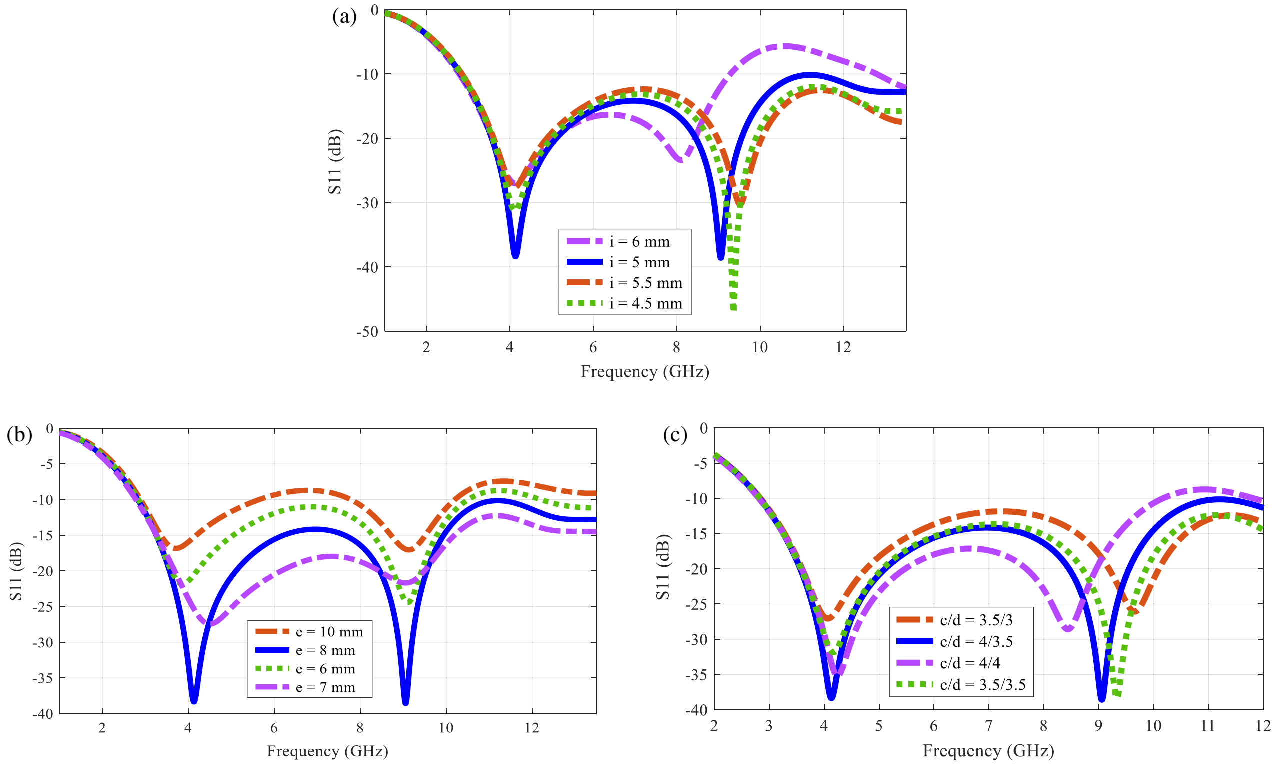

FIGURE 3. Effect of (a) patch slot length (e), (b) ground width (i), and (c) rectangular edge slot dimension on the S_{11}.

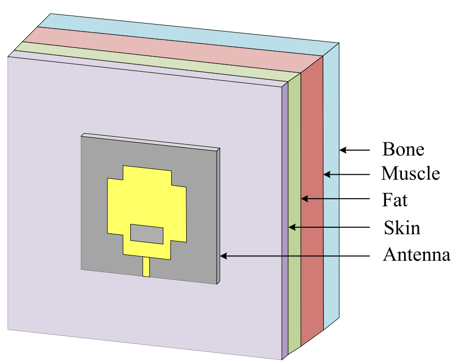

FIGURE 4. Perspective view of the proposed antenna in a human body phantom environment.

TABLE 3. Radiation pattern parameters.

Parameter	5 GHz		9 GHz	
	E-Plane	H-Plane	E-Plane	H-Plane
Main Lobe Mag. (dBi)	2.43	1.86	3.59	1.7
Main Lobe Direction (Deg.)	149	126	139	200
Angular Width (Deg.)	52.6	38.3	48.7	39.1
Side Lobe Level (dBi)	−3.2	−5	−1.3	−1.4

losses due to the finite conductivity of copper and slotting in the patch and defected ground structure. Moreover, proximity to the human body results in electromagnetic absorption and body-loading effects, further reducing radiation efficiency. Nevertheless, the antenna maintains acceptable efficiency over the entire band for WBAN applications.

In addition, Fig. 7 illustrates simulated radiation characteristics of the proposed antenna at 5 GHz and 9 GHz, and the corresponding parameters are outlined in Table 3. Moreover, the variation of gain with respect to frequency is depicted in Fig. 8. The antenna achieved an average gain of 2.36 dBi and a peak gain of 3.79 dBi, demonstrating adequate gain performance over the operating band.

3.2. SAR Analysis of the Proposed Antenna

To evaluate the radiation effect of the proposed UWB antenna on the human body for WBAN applications, SAR was calculated. The SAR analysis was performed by placing the antenna on the human body surface model with an input power of 100 mW (20 dBm) under both 1 g and 10 g tissue standards. The analysis was conducted at 3 GHz, 5 GHz, 7 GHz, and 9 GHz, and corresponding results are illustrated in Fig. 9 and summarized in Table 4. According to the results, the SAR values are within the acceptable standard safety limits of 1.6 W/kg (1 g of tissue) and 2 W/kg (10 g of tissue).

3.3. Bending Analysis of the Proposed Antenna

The proposed antenna was evaluated under different bending conditions to verify its suitability for wearable applications. The results in Fig. 10 show that bending along the XZ-axis does not impact the performance; however, bending along the YZ-axis slightly shifts the lower-band resonances toward lower frequencies. Despite these slight variations, the antenna

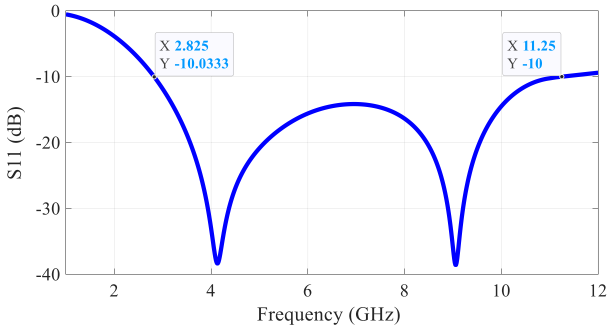

FIGURE 5. Simulated reflection coefficient (S_{11}) of the proposed antenna.

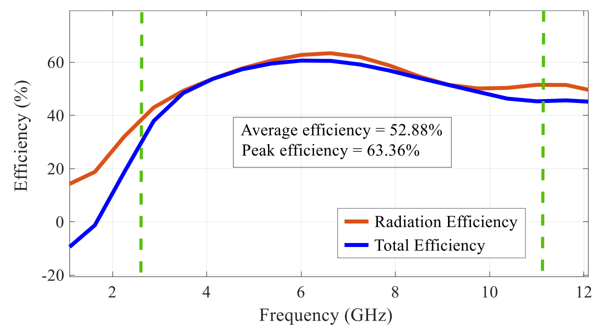

FIGURE 6. Simulated efficiency of the proposed antenna.

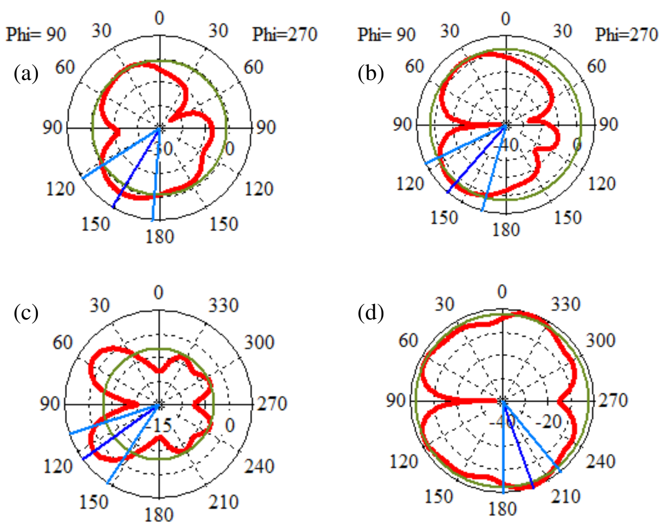

FIGURE 7. 1D radiation pattern at 5 GHz in (a) E-plane and (b) H-plane, and at 9 GHz in (c) E-plane and (d) H-plane.

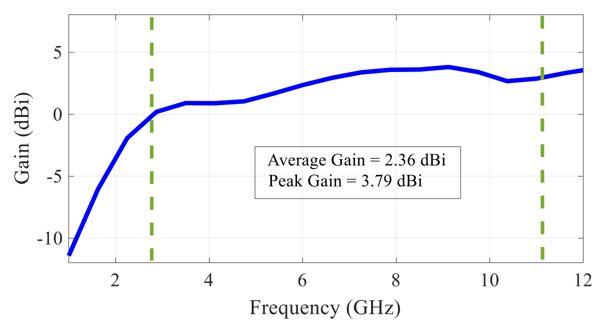

FIGURE 8. Simulated gain of the proposed antenna.

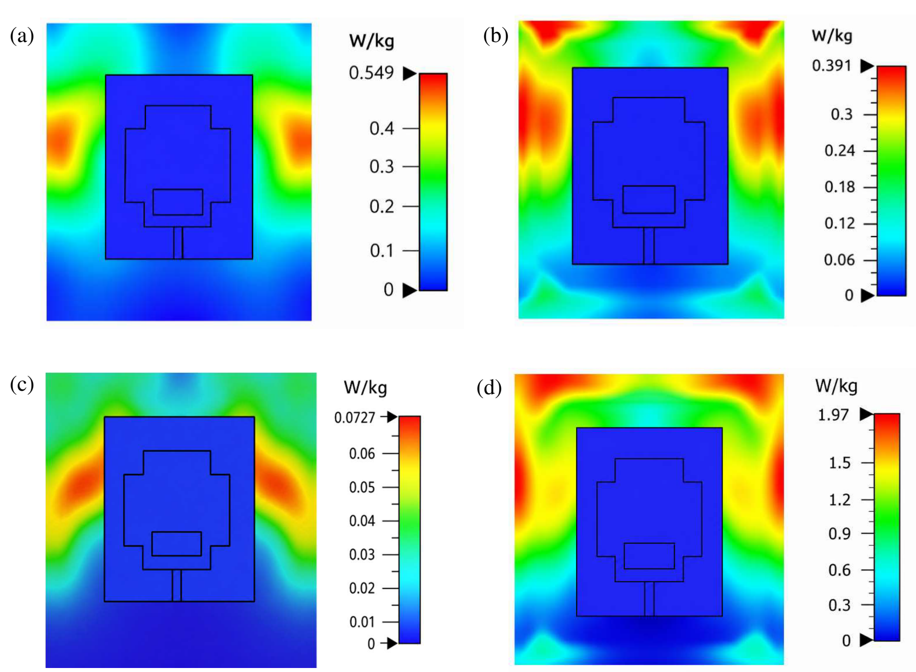

FIGURE 9. SAR analysis of the antenna: (a) 5 GHz, 1 g, (b) 5 GHz, 10 g, (c) 9 GHz, 1 g, (d) 9 GHz, 10 g.

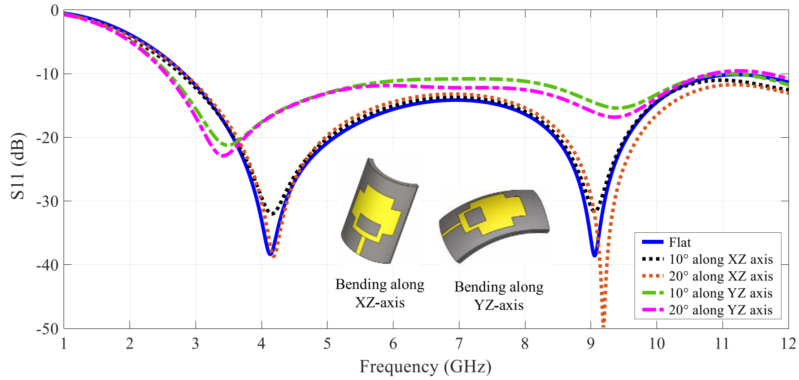

FIGURE 10. Bending analysis of the proposed antenna.

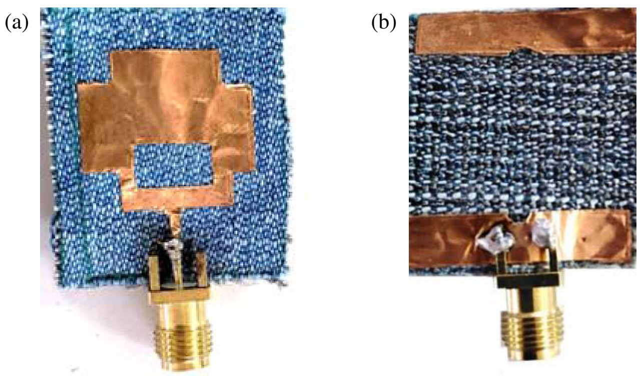

FIGURE 11. (a) Front view and (b) back view of the fabricated proposed antenna.

FIGURE 12. Experimental setup for S_{11} measurement.

TABLE 4. SAR values for 100 mW power in human body model.

Tissue Weight (gm)	Resonant Frequency (GHz)	Maximum SAR (W/kg)
1	3	1.2170
	5	0.5490
	7	0.3110
	9	0.0727
10	3	0.1740
	5	0.3910
	7	1.1810
	9	1.9700

maintained stable wideband performance under all bending conditions with acceptable impedance matching. Therefore, it can be said that the proposed antenna is suitable for flexible WBAN applications.

3.4. Fabrication and Testing of the Proposed Antenna

The proposed UWB wearable antenna was fabricated using jeans fabric as the substrate, and a copper strip was used as a conductive layer. An SMA female connector was soldered to the feed line to provide excitation. The reflection coefficient S_{11} of the antenna was evaluated using a ZNL20 vector network analyzer (VNA) with a frequency range of 5 kHz to 20 GHz. A 3.5 mm male coaxial connector was used to connect the fabricated antenna to the VNA. Fig. 11 presents the fabricated antenna structure, and Fig. 12 illustrates the experimental setup used for S_{11} characterization.

According to the measured results and their comparison with the simulated data, as shown in Fig. 13, the antenna operated over a frequency range of 2.62 GHz to 12.07 GHz. This demonstrates a slight deviation from the simulated bandwidth, which ranges from 2.82 GHz to 11.25 GHz. This variation can be attributed to minor fabrication inaccuracies, potential changes in the dielectric properties of the jeans substrate, effects from connectors and soldering, and external factors during the measurement process. Moreover, the measured results were obtained for various bending conditions, as shown in Fig. 14, demonstrating compliance with the simulated bending results. Nonetheless, the measured results closely matched the simulated performance, confirming the validity of the proposed antenna design for wearable UWB applications.

3.5. Implementation of the Antenna in a WBAN System

To evaluate the proposed antenna's performance in terms of communication reliability for WBAN applications, a prototype human body temperature monitoring system was developed. The system consisted of a DHT22 temperature sensor integrated with an ESP32 microcontroller (NodeMCU ESP32S WiFi module).

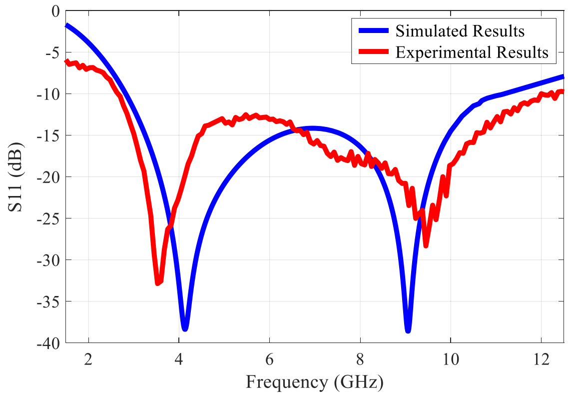

FIGURE 13. Comparison between simulated and measured S_{11} of the proposed antenna.

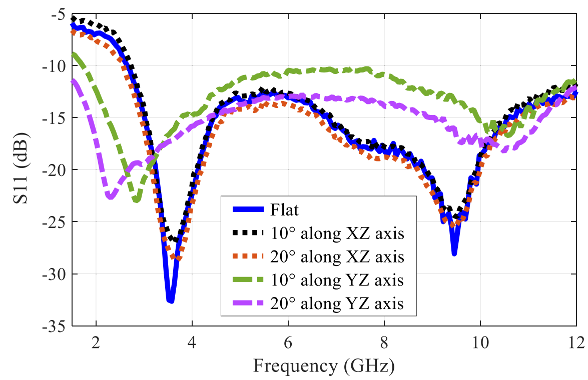

FIGURE 14. Experimental results for various bending conditions.

TABLE 5. Comparative analysis of the proposed antenna model with the existing antenna models.

Ref.	Year	Size (mm^3)	Substrate	Operating Frequency (GHz)	Fractional Bandwidth (%)	Peak Efficiency (%)	Peak Gain (dBi)	SAR (W/Kg)		Comparison with the Proposed Antenna
								1g	10g	
[26]	2025	60 × 60 × 3.85	Rogers 4003C	5.12-9.13	58.65	90	9.4	-	0.065	Higher gain and efficiency, but larger size with smaller bandwidth
[27]	2024	16 × 16 × 0.08	Polyimide	3.15-10.55	128.36	-	4.2	1.99	1.56	Compact size with higher gain, but with smaller bandwidth
[28]	2022	25 × 30 × 1.4	Jeans	3.09-11.00	135.67	65	2.68	0.94	-	Higher gain and efficiency, but larger size with smaller bandwidth
[29]	2022	92× 92 × 1.5	Polyethy-lene	2.00-14.00	226.78	-	7.2	0.001	-	Higher gain and bandwidth, but larger size
[30]	2021	36 × 39 × 2	Jeans	3.00-11.00	139.26	-	6.97	0.29	-	Higher gain, but larger size with lower bandwidth
[31]	2020	10 × 10× 0.37	Jeans	3.96-10.6	102.48	-	5.47	-	1.68	Higher gain and smaller in size, but smaller bandwidth with higher SAR
This Work	2026	23 × 30 × 1.5	Jeans	2.82-11.25	149.67	63.36	3.79	0.621	1.97	Compact size with high bandwidth, adequate gain, efficiency and small SAR

In this prototype, the built-in antenna of the ESP32 microcontroller was replaced with the proposed antenna. The entire temperature monitoring unit was placed on the subject's body to emulate a realistic WBAN deployment in proximity to human tissue, as illustrated in Fig. 15. During testing, the temperature sensor continuously recorded the subject's body temperature and wirelessly transmitted the data through the proposed antenna to the ESP32 server without any interruption. The successful real-time transmission of physiological data confirms that the antenna is suitable for WBAN applications, particularly for wearable health monitoring systems that require compact size, efficient operation near the human body, and reliable wireless communication.

4. COMPARISON WITH THE EXISTING ANTENNAS

Table 5 presents a comparative analysis of the proposed antenna and recent designs. This demonstrates that the proposed antenna achieves a significantly wider bandwidth than the others. Although some existing antennas offer slightly higher gain or efficiency, they generally require larger dimensions or exhibit a higher SAR. In contrast, the proposed antenna maintains an adequate peak gain of 3.79 dBi and a satisfactory peak efficiency of 63.36%, while ensuring significantly lower SAR values of 0.621 and 1.18 W/kg at 5 GHz and 9 GHz frequencies, respectively, with a very high bandwidth of 149.67%. Therefore, the proposed antenna offers a high bandwidth while maintaining compactness, radiation performance, and user safety for wearable and WBAN applications.

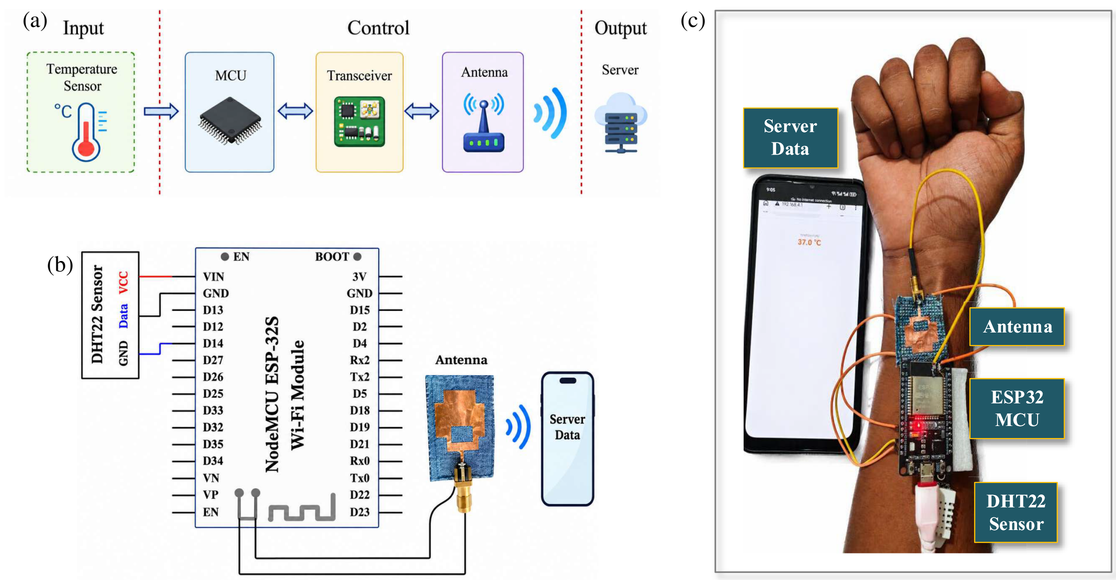

FIGURE 15. (a) Block diagram, (b) connection diagram, and (c) experimental setup of the human body temperature monitoring system using the proposed antenna.

5. CONCLUSION

This study presents a novel low-profile UWB wearable antenna, specifically designed for WBAN applications. The antenna is fabricated on a flexible jeans substrate with integrated patch slots and a DGS, which successfully demonstrates a wide operating frequency range of 2.82–11.25 GHz with a compact size of $23 \times 30 \times 1.5\,\text{mm}^3$. The simulation results indicated satisfactory impedance matching, a peak gain of 3.79 dBi, average gain of 2.36 dBi, peak efficiency of 63.36%, and average efficiency of 52.88%, while maintaining SAR values within standard safety limits for 1 g and 10 g tissues. Bending analyses validated the antenna's stable performance under various deformation conditions, supporting its suitability for flexible and wearable applications. The fabrication and experimental validation on a human body showed close agreement with the simulated results, achieving an operational bandwidth of 2.62–12.07 GHz. Furthermore, practical implementation in a human body temperature monitoring system using a DHT22 sensor and ESP32 microcontroller demonstrated reliable real-time data transmission, thus validating the antenna's efficacy in WBAN deployment.

Compared with existing wearable antennas, the proposed design achieves a strong balance of wide bandwidth, compact size, adequate gain and efficiency, and low SAR. Overall, the proposed antenna represents a significant advancement in UWB WBAN applications, particularly in health monitoring and other wearable IoT systems.

ACKNOWLEDGEMENT

This work was supported in part by the Ministry of Higher Education (MOHE) through the Fundamental Research Grant Scheme (FRGS) via Universiti Teknikal Malaysia Melaka under Grant FRGS/1/2025/TK07/UTEM/02/3.

REFERENCES

[1] Sethuraman, S. C., P. Kompally, S. P. Mohanty, and U. Choppali, "MyWear: A novel smart garment for automatic continuous vital monitoring," *IEEE Transactions on Consumer Electronics*, Vol. 67, No. 3, 214–222, Aug. 2021.

[2] Kulkarni, M. B., S. Rajagopal, B. Prieto-Simón, and B. W. Pogue, "Recent advances in smart wearable sensors for continuous human health monitoring," *Talanta*, Vol. 272, 125817, May 2024.

[3] Abdi, A., F. Ghorbani, H. Aliakbarian, T. K. Geok, S. K. A. Rahim, and P. J. Soh, "Electrically small spiral PIFA for deep implantable devices," *IEEE Access*, Vol. 8, 158 459–158 474, 2020.

[4] Alqadami, A. S. M., K. S. Bialkowski, A. T. Mobashsher, and A. M. Abbosh, "Wearable electromagnetic head imaging system using flexible wideband antenna array based on polymer technology for brain stroke diagnosis," *IEEE Transactions on Biomedical Circuits and Systems*, Vol. 13, No. 1, 124–134, Feb. 2019.

[5] Al Rasyid, M. U. H., B.-H. Lee, and A. Sudarsono, "Wireless body area network for monitoring body temperature, heart beat and oxygen in blood," in *2015 International Seminar on Intelligent Technology and Its Applications (ISITIA)*, 95–98, Surabaya, Indonesia, May 2015.

[6] Singh, M. and N. Jain, "Performance and evaluation of smartphone based wireless blood pressure monitoring system using Bluetooth," *IEEE Sensors Journal*, Vol. 16, No. 23, 8322–8328, Dec. 2016.

[7] Qu, L., R. Zhang, and H. Kim, "High-sensitivity ground radiation antenna system using an adjacent slot for Bluetooth headsets," *IEEE Transactions on Antennas and Propagation*, Vol. 63, No. 12, 5903–5907, Dec. 2015.

[8] Hong, S., S. H. Kang, Y. Kim, and C. W. Jung, "Transparent and flexible antenna for wearable glasses applications," *IEEE Transactions on Antennas and Propagation*, Vol. 64, No. 7, 2797–2804, Jul. 2016.

[9] Alqadami, A. S. M., A. Trakic, A. E. Stancombe, B. Mohammed, K. Bialkowski, and A. Abbosh, "Flexible electromagnetic cap for head imaging," *IEEE Transactions on Biomedical Circuits and

Systems, Vol. 14, No. 5, 1097–1107, Oct. 2020.

[10] Lee, H., H. Yang, S. Myeong, and K. Lee, "Dual-band MNG patch antenna for smart helmet," *Electronics Letters*, Vol. 54, No. 19, 1101–1102, Sep. 2018.

[11] Chen, Y.-S. and T.-Y. Ku, "A low-profile wearable antenna using a miniature high impedance surface for smartwatch applications," *IEEE Antennas and Wireless Propagation Letters*, Vol. 15, 1144–1147, 2016.

[12] Modak, S. and T. Khan, "A slotted UWB-MIMO antenna with quadruple band-notch characteristics using mushroom EBG structure," *AEU — International Journal of Electronics and Communications*, Vol. 134, 153673, May 2021.

[13] Federal Communications Commission, "Revision of Part 15 of the commission's rules regarding ultra-wideband transmission systems," Tech. Rep., FCC 02-48, First Report Order, Washington, DC, USA, 2002.

[14] Meena, M. L., M. Kumar, G. Parmar, and R. S. Meena, "Design analysis and modeling of directional UWB antenna with elliptical slotted ground structure for applications in C- & X-bands," *Progress In Electromagnetics Research C*, Vol. 63, 193–207, 2016.

[15] Eshtiaghi, R., J. Nourinia, and C. Ghobadi, "Electromagnetically coupled band-notched elliptical monopole antenna for UWB applications," *IEEE Transactions on Antennas and Propagation*, Vol. 58, No. 4, 1397–1402, Apr. 2010.

[16] Abbosh, A. M. and M. E. Bialkowski, "Design of ultrawideband planar monopole antennas of circular and elliptical shape," *IEEE Transactions on Antennas and Propagation*, Vol. 56, No. 1, 17–23, Jan. 2008.

[17] Rahanandeh, M., A. S. N. Amin, M. Hosseinzadeh, P. Rezai, and M. S. Rostami, "A compact elliptical slot antenna for covering Bluetooth/WiMAX/WLAN/ITU," *IEEE Antennas and Wireless Propagation Letters*, Vol. 11, 857–860, 2012.

[18] Angelopoulos, E. S., A. Z. Anastopoulos, D. I. Kaklamani, A. A. Alexandridis, F. Lazarakis, and K. Dangakis, "Circular and elliptical CPW-fed slot and microstrip-fed antennas for ultrawideband applications," *IEEE Antennas and Wireless Propagation Letters*, Vol. 5, 294–297, 2006.

[19] Yan, Y.-D., Y.-C. Jiao, Z. Weng, and C. Zhang, "An umbrella-shaped broadband circularly polarized antenna with wide beamwidth for global navigation satellite systems applications," *Microwave and Optical Technology Letters*, Vol. 61, No. 11, 2455–2462, Nov. 2019.

[20] Kundu, S., A. Chatterjee, S. K. Jana, and S. K. Parui, "A compact umbrella-shaped UWB antenna with gain augmentation using frequency selective surface," *Radioengineering*, Vol. 27, No. 2, 448–454, Jun. 2018.

[21] Elsheakh, D. N., H. A. Elsadek, E. A. Abdallah, M. F. Iskander, and H. Elhenawy, "Ultrawide bandwidth umbrella-shaped microstrip monopole antenna using spiral artificial magnetic conductor (SAMC)," *IEEE Antennas and Wireless Propagation Letters*, Vol. 8, 1255–1258, 2009.

[22] Paracha, K. N., S. K. A. Rahim, P. J. Soh, and M. Khalily, "Wearable antennas: A review of materials, structures, and innovative features for autonomous communication and sensing," *IEEE Access*, Vol. 7, 56 694–56 712, 2019.

[23] Sankaralingam, S. and B. Gupta, "Determination of dielectric constant of fabric materials and their use as substrates for design and development of antennas for wearable applications," *IEEE Transactions on Instrumentation and Measurement*, Vol. 59, No. 12, 3122–3130, Dec. 2010.

[24] Rahman, A., M. T. Islam, M. J. Singh, S. Kibria, and M. Akhtaruzzaman, "Electromagnetic performances analysis of an ultra-wideband and flexible material antenna in microwave breast imaging: To implement a wearable medical bra," *Scientific Reports*, Vol. 6, No. 1, 38906, Dec. 2016.

[25] Klemm, M. and G. Troester, "Textile UWB antennas for wireless body area networks," *IEEE Transactions on Antennas and Propagation*, Vol. 54, No. 11, 3192–3197, Nov. 2026.

[26] Li, X., Z. Zhou, K. Wang, Y. Yang, Z. Pang, X. Zhou, W. Tang, Z. Huang, and D. Lan, "UWB metasurface antenna with improved gain and bandwidth for WBAN application," *IEEE Transactions on Consumer Electronics*, Vol. 71, No. 2, 5465–5474, May 2025.

[27] Kanagasabai, M., P. Sambandam, M. G. N. Alsath, S. Palaniswamy, A. Ravichandran, and C. Girinathan, "Miniaturized circularly polarized UWB antenna for body centric communication," *IEEE Transactions on Antennas and Propagation*, Vol. 70, No. 1, 189–196, Jul. 2022.

[28] Modak, S., V. Kaim, T. Khan, B. K. Kanaujia, L. Matekovits, and K. Rambabu, "Design and performance measurement of worn-on-body instrumental ultra-miniaturized UWB wearable patch for e-health monitoring," *IEEE Access*, Vol. 12, 25 719–25 730, Feb. 2024.

[29] Jayant, S., G. Srivastava, and S. Kumar, "Quad-port UWB MIMO footwear antenna for wearable applications," *IEEE Transactions on Antennas and Propagation*, Vol. 70, No. 9, 7905–7913, Sep. 2022.

[30] Parameswari, S. and C. Chitra, "Textile UWB antenna with metamaterial for healthcare monitoring," *International Journal of Antennas and Propagation*, Vol. 2021, No. 1, 5855626, Dec. 2021.

[31] Yadav, A., V. K. Singh, A. K. Bhoi, G. Marques, B. Garcia-Zapirain, and I. de la Torre Díez, "Wireless body area networks: UWB wearable textile antenna for telemedicine and mobile health systems," *Micromachines*, Vol. 11, No. 6, 558, May 2020.

[32] Douhi, S., S. Labihi, A. Eddiai, S. Lakrit, M. El Achaby, and A. J. A. Al-Gburi, "Design, characterization, and electromagnetic performance of a flexible wideband RF antenna using composite materials," *Journal of Science: Advanced Materials and Devices*, Vol. 10, No. 1, 100847, 2025.

[33] Zhang, M., P. Xu, H. Peng, and F. Qin, "A rational design of core-shell-satellite structured $BaTiO_3$ fillers for epoxy-based composites with enhanced microwave dielectric constant and low loss," *Composites Part B: Engineering*, Vol. 215, 108764, 2021.

[34] Zhang, S., J. Zhu, Y. Zhang, Z. Chen, C. Song, J. Li, N. Yi, D. Qiu, K. Guo, C. Zhang, *et al.*, "Standalone stretchable RF systems based on asymmetric 3D microstrip antennas with on-body wireless communication and energy harvesting," *Nano Energy*, Vol. 96, 107069, 2022.

[35] Al-Gburi, A. J. A., N. H. M. Radi, T. Saeidi, N. J. Mohammed, Z. Zakaria, G. S. Das, A. Buragohain, and M. M. Ismail, "Superconductive and flexible antenna based on a tri-nanocomposite of graphene nanoplatelets, silver, and copper for wearable electronic devices," *Journal of Science: Advanced Materials and Devices*, Vol. 9, No. 3, 100773, 2024.

[36] Balanis, C. A., *Antenna Theory: Analysis and Design*, 3rd ed., John Wiley & Sons, New York, NY, USA, 2005.